PHYSICAL REVIEW A VOLUME 18, NUMBER 3 SEPTEMBER 1978

Fine structure of the field autocorrelation function of a laser in the threshold region

A. Güttner,* H. Welling, K. H. Gericke, and W. Seifert
Institut für Angewandte Physik, Technische Universität Hannover, 3000 Hannover, Welfengarten 1, Federal Republic of Germany
(Received 1 December 1977)

Autocorrelations due to natural phase and amplitude fluctuations of the laser field were investigated in the threshold region of a 633-nm He-Ne single-mode laser by use of an interferometric autodyne method. The measured time-dependent autocorrelation function shows deviations from an exponential decay that can be described by a formal fine structure predicted by the theoretical Van der Pol laser model. As a consequence, the natural laser spectrum is not exactly Lorentz shaped. The natural linewidth shows the expected general reciprocal power dependence and an additional factor-of-2 narrowing above threshold, in full agreement with the theory.

I. INTRODUCTION

According to theoretical treatments,[1-8] a single-mode laser near threshold behaves like a rotating-wave Van der Pol oscillator, driven by Markovian random forces, which represent the inherent quantum fluctuations. Because of the cubic term in the Langevin equation for the complex amplitude of the electromagnetic field, the field correlation functions of any order in the Glauber representation do not show a simple exponential decay. Rather, they are expressed by sums of weighted exponential terms. The individual relaxation rates and weight factors are in general complex; they are real in the special cases of pure intensity correlations and vanishing detuning.[5]

The parameters have been computed in proper normalization for the autocorrelation functions of the complex-field amplitude and the intensity fluctuations, also termed first-order field correlation function and second-order intensity correlation function, by Risken *et al.*[2,4,5] and Hempstead and Lax.[7] A comparison of these theoretical results with corresponding experimental findings is well suited to verify the validity of the Van der Pol laser model since the numerical values of the parameters reflect the special form of the important nonlinear term in the Langevin equation.

Measurements of the intensity correlation function slightly above threshold by Chopra and Mandel[9] show the predicted nonexponential behavior. Chopra and Dudeja[10] present weight factors and relaxation rates of the two strongest exponential terms computed from these data for twice the threshold power.[11] Corti *et al.*[12] used a refined technique, utilizing distortions in an "imperfect" digital correlator, to enhance the influence of the weaker terms. They measured up to four relaxation rates for different operating points in the threshold region. Owing to the distortions, they did not obtain the weight parameters.

These measurements of second-order intensity correlations as well as measurements of third-order intensity correlations by Chopra and Mandel[13] and Corti and Degiorgio[14] are in good accord with the Van der Pol model of the laser. A further excellent and by far more comprehensive corroboration results from measurements of the photocount distribution for intermediate times and some of its factorial moments by Meltzer *et al.*[15] and Jakeman *et al.*[16] These quantities involve intensity correlations of all orders.[8]

The above-mentioned experiments as well as almost all additional experiments in the threshold region are confined to the anlysis of intensity fluctuations. Therefore, they have not yielded information about phase fluctuations and their coupling with amplitude fluctuations owing to nonlinear mechanisms. To our knowledge, the only exception to date has been Fourier spectroscopic measurements of the natural linewidth by Gerhardt *et al.*[17] Because of the limited resolution of these measurements, no attempt was made to show the predicted small deviations from the exponential decay of the autocorrelation function. An approximation by a single exponential for short delay times should, however, cause distortions of the linewidth values as has been pointed out by Seybold and Risken.[5] The agreement of the measured with the theoretical results above threshold therefore indicates a certain discrepancy between experiment and theory.[5]

To clarify this point and to enhance our understanding of the statistical properties of laser light, we have performed highly accurate measurements of the field autocorrelation function throughout the threshold region, which became possible by decisive methodic and apparative improvements. The experimental results are fully compatible with the Van der Pol laser model. Before describing the measurements and their results in detail, we shall give a short survey of the theoretical behav-

ior of some autocorrelation-function parameters and of experimental problems and solutions.

II. THEORETICAL RESULTS

The purpose of this chapter is the presentation of quantities needed for later considerations; a complete review of theoretical methods and results is not intended.

Under the usual assumptions,[8] the statistical properties of the laser field near threshold are fully described by the following classical Langevin equation of the Van der Pol type (in a rotating frame)[1-4,6-8]:

$$\dot{u}(t) - [a - u^*(t)u(t)]u(t) = F(t) . \tag{1}$$

It is derived for the undetuned case, which shall be assumed throughout this paper. In Eq. (1)

$$u(t) = [r + \rho(t)]e^{i\phi(t)} \tag{2}$$

is the slowly varying complex amplitude of the rapidly oscillating electric field

$$E(t) = u(t)e^{-\omega_0 t} + u^*(t)e^{i\omega_0 t} . \tag{3}$$

Both the amplitude $\hat{u}(t) = r + \rho(t)$ (with $r = \langle \hat{u}(t) \rangle$) and the phase $\phi(t)$ fluctuate under the influence of the Markovian random force $F(t)$. The pump parameter a determines the operating point of the laser. It is proportional to the inversion and therefore related to the pump rate. The laser is at threshold for $a = 0$, below for $a < 0$, and above for $a > 0$. For practical reasons, we shall characterize the operating point by the relative laser power $p = P/P_{\text{threshold}}$, which is rigorously connected with the pump parameter.[7]

All quantities in Eqs. (1)–(4) are normalized by proper scaling for numerical purposes. The unnormalized amplitude and time, marked by over bars, are given by

$$\bar{u} = u\sqrt{B}, \quad \bar{t} = t/C \tag{4}$$

with

$$B = \sqrt{q/\beta}, \quad C = \sqrt{q\beta} . \tag{5}$$

The saturation parameter β and the diffusion parameter q are laser constants that appear in the unnormalized Langevin equation.[1-4] In the following we are mainly concerned with normalized quantities because these are easier to obtain and also show the relevant properties. The scaling factors may be deduced from experimental data.

The calculation of correlation functions of the field is strongly complicated by the nonlinear term in Eq. (1). It is possible by use of a Fokker-Planck equation technique based on the numerical solution of an associated eigenvalue problem.[3-5,7] From the computed stationary joint distribution function $W_2(u, u', \tau)$ all correlation functions are available by simple integration.

Our present interest concentrates on the field autocorrelation function

$$G(p, \tau) = \langle u^*(t + \tau)u(t) \rangle = \int\int\int\int u^* u' \, W_2(u, u', \tau) \, d^2u \, d^2u' , \tag{6}$$

especially the normalized form

$$g(p, \tau) = G(p, \tau)/G(p, 0) , \tag{7}$$

which shows the multiexponential structure mentioned above[5,7]

$$g(p, \tau) = \sum_{m=0}^{\infty} V_m(p) e^{-\lambda_m(p)\tau}, \quad \tau \geq 0 . \tag{8}$$

All weight factors V_m and relaxation rates λ_m are real and positive. From the autocorrelation function the normalized spectral profile $s(p, \omega)$ is obtained as usual by a Fourier transform. Therefore, the spectrum shows an analogous fine structure. It is represented by a series of weighted Lorentz lines with the common center frequency ω_0 and the linewidths λ_m (half width at half power):

$$s(p, \omega) = \sum_{m=0}^{\infty} Y_m \left[1 + \left(\frac{\omega - \omega_0}{\lambda_m} \right)^2 \right]^{-1} . \tag{9}$$

The weight factors Y_m are related to V_m and λ_m

$$Y_m = V_m \frac{\lambda_{\text{eff}}}{\lambda_m}, \quad \lambda_{\text{eff}} = \sum_{m=0}^{\infty} \left(\frac{V_m}{\lambda_m} \right)^{-1} . \tag{10}$$

λ_{eff} is the effective linewidth of the non-Lorentzian spectrum; it does not differ significantly from λ_0 because V_0 and Y_0 are always greater than 0.97 or 0.997, respectively.

In Fig. 1 we have summarized some of the numerical results concerning first-order correlations, in order to give an impression of the operation point dependence of the parameters and their interrelations. The linewidth of the dominating term λ_0 shows essentially the $1/p$ dependence known from the Schawlow-Townes formula for the natural linewidth. The deviation from a pure $1/p$ slope is characterized by the variation of the linewidth factor α_0 in the threshold region. α_0 and the analogous quantity α_{eff}, related to the effective linewidth, are defined by

$$\alpha_0 = 2p\lambda_0/\sqrt{\pi}, \quad \alpha_{\text{eff}} = 2p\lambda_{\text{eff}}/\sqrt{\pi} . \tag{11}$$

Unlike λ_0, higher-order linewidth parameters are possessing minima near threshold. For rising index m, the values of λ_m increase monotonously, whereas the weight factors V_m and Y_m decrease in general, Y_m by far faster than V_m. The contribu-

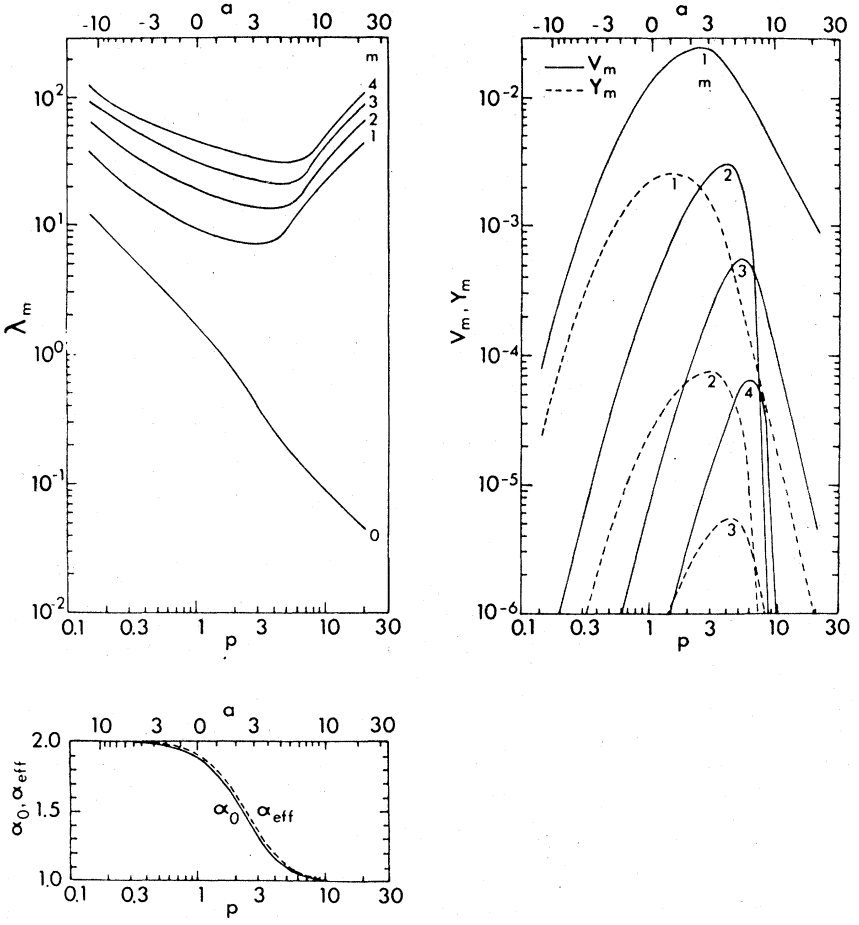

FIG. 1. Theoretical values of the fine-structure parameters λ_m, V_m, and Y_m and of the linewidth factors α_0 and α_{eff} deduced from Refs. 3 and 6.

tions of the higher-order terms reach maxima slightly above threshold, but they remain very small also in this region. Their influence on certain quantities, e.g., the slope of the autocorrelation function for $\tau \to 0$, may be considerable, nevertheless, even far from threshold.[5]

III. SELECTION AND DISCUSSION OF THE EXPERIMENTAL METHOD

Following the theoretical results cited above, the natural laser spectrum in general consists of a high, narrow line and a weak background composed of flat, broad lines. An experimental proof of this fine structure is by no means a trivial spectroscopic problem, for various reasons:

(i) The natural line is too narrow—one has to expect linewidth values in the range ~10^2–~10^4 Hz—to be resolvable by standard spectroscopic methods.

(ii) Deviations from a pure Lorentzian can only be detected if the laser line is measured precisely at least three orders of magnitude below its maximum.

(iii) Fluctuations and disturbances not caused by quantum noise, so-called technical noise,[22] result in an additional Gaussian broadening of the laser line, which may exceed the natural one by far.

(iv) The technical noise is in general nonstationary, so that the technical linewidth is subject to temporal variations.

Therefore, a careful selection of the method of investigation is necessary.

Doubtless, the strong resolution requirements can be best fulfilled by heterodyne methods because the high spectral resolving power is furnished by electronic means. Siegman *et al.* described in a fundamental paper[18] three different ways to analyze the beat signal, which have all been successfully employed in the meantime to investigate the natural linewidth of lasers above threshold.[19-23] The two methods used in most cases are based exclusively on the analysis of phase fluctuations, especially of the spectral power density of the instantaneous laser frequency $\dot{\phi}$ and of the averaged quadratic phase jitter $\langle \Delta\phi^2(\tau) \rangle$. Amplitude fluctuations are not interpreted correct-

ly; therefore these methods fail near and below threshold where the amplitude is not stabilized.

Not restricted, in principle, with respect to the laser operating point, are methods which consider the spectral power density or (not discussed in Ref. 18) the autocorrelation function of the ac component of the detector signal, respectively.[24] There are, however, practical reasons that affect the suitability of these methods for the present problem. In addition to the beat signal, the detector signal comprises contributions owing to intensity fluctuations (of both the signal and the reference laser), shot noise, dark current noise, and noise in the electronic system. All these noise sources give rise to additive terms, which have to be measured separately for the purpose of corrections. Because the spectra of the interfering noise contributions are broad in general, it may be very difficult to resolve the natural fine structure, especially by means of the spectral method.

Although the knowledge of the power spectrum is equivalent to that of the autocorrelation function from a theoretical point of view, Fourier spectroscopic methods offer some experimental advantages in our case. As shown in Fig. 1, weight factors are shifted in favor of weaker terms and technical noise suppresion is made easier. The vital information of the wings of the spectrum is transformed mainly into the maximum of the autocorrelation function and thus into the range best accessible by experiments.

This feature of the autocorrelation function is of special importance with respect to methods based on the autodyne principle, because in this case the resolution is limited by the attainable interferometer path differences.

Fourier spectrometers measuring the normalized field autocorrelation function[25] $\gamma(\tau)$ [in contrast to $g(\tau)$, $\gamma(\tau)$ includes the influence of the additional technical fluctuations] are restricted to path differences of several meters owing to the extreme precision requirements. The attainable resolving power does not suffice to analyze the small laser lines, by far.

The requirements are strongly reduced, if instead of the oscillating interferogram $\gamma(\tau)$ its slowly varying envelope $|\gamma(\tau)|$ is measured, which is closely related to the visibility. By use of multiply folded rays, path lengths of some kilometers corresponding to delay times of some microseconds are attainable under laboratory conditions. The lack of information about the phase of the autocorrelation function does not affect the reconstruction of the spectrum in the case of symmetrical spectra as considered throughout this paper.

Without any *a priori* information about the spectrum, the smallest resolvable linewidth $\Delta\nu$ of a He-Ne laser computed for a maximum path difference Δs_{max} of 2000 m is 75 kHz, a value by far greater than the linewidths to be measured. However, the effective resolution is enhanced considerably by reasonable assumptions about the lineshape, so that measurements in the kilohertz range are possible. None of the methods considered above are free from shortcomings of a principal or practical nature. The analysis of the fine structure via the visibility is preferred for the following reasons:

(a) Noise contributions (shot noise, amplifier noise, intensity fluctuations) cause fluctuations around the mean value, which can be made as small as necessary by means of a sufficiently high time constant.

(b) The resolution is the greater the closer the normalized field autocorrelation function approaches the value 1 (see below). In a certain sense it is fitted automatically to the actual accuracy requirements.

(c) Problems connected with the additional reference laser and the difference frequency stabilization are avoided.

The autodyne method to be described is not new in its basic concept[25] and needs not be repeated here. We shall therefore restrict ourselves to some specific aspects connected with the present measuring problem.

The visibility $V(\tau)$ of an interference figure is defined by

$$V(\tau) = (I_{max} - I_{min})/(I_{max} + I_{min}), \tag{12}$$

where I_{max} and I_{min} are the maximum and minimum averaged intensities, respectively, measured at one observation point for two suitable values of the interferometer phase. In the special case of equal identities I_1 and I_2 of the interfering beams, the modules $|\gamma(\tau)|$ of the normalized field autocorrelation function is identical with $V(\tau)$. In general, the relation

$$|\gamma(\tau)| = \frac{I_1 + I_2}{2(I_1 I_2)^{1/2}} V(\tau) \tag{13}$$

is valid. In the case of symmetrical lines considered here $|\gamma(\tau)|$ coincides with $\gamma(\tau)$. Therefore, the signs for the modules are omitted in the following.

For optical fields showing nonstationary phase fluctuations it is more reasonable from a simple error analysis to use only one of the extreme values I_{max} and I_{min} (which are fluctuating quantities in this case) for computing $\gamma(\tau)$. The measurements we made were based on the formulas

$$\gamma(\tau) = (I_1 + I_2 - I_{min})/2(I_1 I_2)^{1/2} \tag{14}$$

$$\gamma(\tau)=1-2I_{\min}/\{I_{\max}+I_{\min}\},\quad I_1=I_2 \tag{15}$$

which are used under different experimental conditions. Obviously, measurements according to Eq. (15) instead of Eq. (12) are only of advantage, if the essentially stable expression $\{I_{\max}+I_{\min}\}$ is determined directly, i.e., without measuring the fluctuating individual terms. Details of the experimental realization are given in Sec. IV.

The effective-field spectrum of the laser light has to be considered as a convolution of the natural spectrum and the Gaussian spectrum owing to technical disturbances of the laser and the interferometer. The observed autocorrelation function $\gamma(p,\tau)$ is therefore the product of the Fourier transforms of both spectra:

$$\gamma(p,\tau)=\epsilon g(p,\tau)h(p). \tag{16}$$

$g(p,\tau)$ and $h(\tau)$ are the individual normalized autocorrelation functions connected with the natural and the technical fluctuations, respectively. The additional factor ϵ $(0<\epsilon<1)$ takes into account the systematic error in the analysis of the interference figure owing to a finite measurement area. As can be shown, ϵ does not depend on the visibility and hence on the operating point p and the delay time τ. Assuming a well-designed operating-point stabilization system, the function $h(\tau)$ is independent of p as well. Consequently, the elimination of the inconvenient factors ϵ and $h(\tau)$ in Eq. (16) is simply achieved by a double measurement technique. The desired quantity is given by

$$g(p,\tau)=g(p_r,\tau)[\gamma(p,\tau)/\gamma(p_r,\tau)], \tag{17}$$

where p_r is a relative reference power different from p. The problem is thus shifted to the determination of $g(p_r,\tau)\equiv g_r$. For $p_r\gg p,1$, the assumption $g_r=1$ is justified because of the $1/p$ dependence of the natural linewidth; in general, however, more exact values of g_r are required. A reasonable first step is the approximation of g_r by the theoretical value given by Eq. (8). If necessary, improvements by interative means can be made.

In addition to technical disturbances, the light intensities to be measured are affected by shot noise and natural intensity fluctuations resulting in an upper limit of the obtainable resolutior, which depends on the experimental situation.

Assuming $I_1\simeq I_2\simeq\frac{1}{4}I_{\max}$, the relative uncertainty of the measured value $\gamma(p,\tau)$ is given by

$$r(\gamma)=\frac{1-\gamma}{\gamma}\left[\left(2+\frac{1}{2(1-\gamma)}\right)r_s^2(I_1)+3r_i^2(I_1)\right]^{1/2} \tag{18a}$$

$$\simeq\left(\frac{1-\gamma}{2}\right)^{1/2}r_s(I_1),\quad 1-\gamma\ll 1. \tag{18b}$$

$r(x)$ represents the expression $\sigma(x)/x$, where $\sigma(x)$ is the standard deviation of a quantity x. The subscripts s and i indicate the contributions of shot noise and natural intensity fluctuations, respectively.

It is evident from Eq. (18b) that the signal-to-noise ratio is the larger, the closer γ approximates the value 1. This is important because the decay of the autocorrelation function is not very pronounced in our experiments owing to the small delay times and linewidths.

It should be mentioned that this favorable behavior is not characteristic for the visibility method in general. Measurements according to the formula

$$\gamma(\tau)=(I_{\max}-I_1-I_2)/2(I_1I_2)^{1/2} \tag{19}$$

result in a signal-to-noise ratio that is by a factor $\geq(20/[1-\gamma])^{1/2}$ lower for $\gamma\to 1$, i.e., by several orders of magnitude. Equation (19) is very similar to Eq. (14) and is obtained in an equivalent manner.

The values $r_s(I_1)$ and $r_i(I_1)$ in Eq. (18) are found by considering the relative noise power in the frequency range $0\leq f\leq(4T)^{-1}$ determined by the average time constant T:

$$r_s^2(I_1)=\frac{h\nu\Gamma^2}{\pi T\eta[0.5k(\tau)R^{n(\tau)}P_{\text{thr}}p]}, \tag{20}$$

$$r_i^2(I_1)=\frac{r_r^2(p)}{2TC\Lambda_{\text{eff}}(p)}. \tag{21}$$

In Eq. (20) η is the quantum efficiency of the photocathode and Γ the shot-noise enhancement factor of the photomultiplier. $R^{n(\tau)}$ allows for the intensity loss due to the multiple reflections in the delay line [R is the reflection coefficient and $n(\tau)$ the number of reflections] and $k(\tau)$ allows for all losses between laser and detector by other reasons. The values of $\Lambda_{\text{eff}}(p)$, the normalized effective width of the spectrum of the natural intensity fluctuations, and $r_r^2(p)\cong\langle\rho^2(t)\rangle/r^2$ in Eq. (21) can be drawn from Ref. 7. C is the scaling factor defined in Eq. (5).

To give a realistic impression of the theoretical resolution, we present in Table I the calculated signal-to-noise ratios for different operating points and path differences under the conditions of our

TABLE I. Theoretical signal-to-noise ratio owing to shot noise and natural intensity fluctuations for different laser operating points and optical path lengths.

Δs [m]	p 0.2	1	4	20
80	1×10^4	3×10^4	1×10^5	3×10^5
500	2×10^3	8×10^3	3×10^4	1×10^5
2000	4×10^1	3×10^2	1×10^3	3×10^3

experiments. The influence of the technical noise and the finite measurement area is taken into account using Eq. (16), whereby the values of ϵ and $h(\tau)$ were deduced from the experimental data.

IV. MEASURING EQUIPMENT

For the practical realization of the experimental concept outlined in the preceding sections, two aspects are essential. First the measuring equipment has to be suited for measurements near the theoretical resolution limit, a problem mainly concerning the electronic system, and further, the multiple external disturbances have to be eliminated or at least diminished by a highly stable optical system, by effective shieldings and, last not least, by use of a laser with anomalously strong natural fluctuations reducing the disturbing influence of the remaining technical noise.

Figure 2 shows a schematic diagram of the measuring system. Essentially, it consists of the signal source, a 633-nm single-mode He-Ne laser, and the field correlator being composed of a Mach-Zehnder interferometer with an internal optical delay line, a photomultiplier and the electronic system.

The laser has been developed especially in regard to our experiments. Compared with commercial single-mode He-Ne lasers, it offers a threshold at least the threefold natural linewidth and approximately the twofold output power. Noise problems concerning the visibility measurement, the threshold determination and the operating-point stabilization are effectively reduced. In Table II we present some data and parameters of the laser that may be of interest; it was, however, not the aim of this work to determine their values with maximum accuracy.

The control of the laser operating point is achieved by shifting the cavity frequency within the gain profile. The required detuning is always small enough to be neglected. Other possible methods are connected with more aggravating problems as greater changes of the parameters β and q and variations of the discharge noise, which exclude the elimination procedure discussed in Sec. III. The resonator detuning is accomplished as usual by a piezoceramic translator ($PC1$) shifting one of the resonator mirrors. A servo system stabilizes the operating point during the measurement.

The exact knowledge of the operating point follows from measurements of the spectral-power density of the intensity fluctuations near zero frequency, $S_{\Delta I}(0)$. This quantity shows a clear operating-point dependence as can be seen in Fig. 3, which also explains the identification of the threshold.

With the available mirrors (radius of curvature 2 m, reflection coefficient 99.4%) the folded optical

TABLE II. Data and parameters of the He-Ne laser.

Discharge tube	
Inner diameter	0.6 mm
Active length	104 mm
Gas pressure	4.6 Torr
He-Ne ratio	8.2:1
Isotope structure	Natural mixtures
Discharge current	4.0 mA
Resonator	
Mirror spacing	153 mm
Radii of curvature	147 mm
Transmissivity, output mirror	$(5.8 \pm 0.8)\%$
Roundtrip loss	$(9 \pm 1)\%$
Cavity linewidth	$(1.45 \pm 0.2)10^7$ Hz
Laser parameters	
Diffusion parameter	$(9 \pm 1)10^7$ sec^{-1}
Saturation parameter	(2.3 ± 0.3) sec^{-1}
Number of noise photons	2.0 ± 0.5
Threshold data	
Output power	$(1.3 \pm 0.1)10^{-7}$ W
Photon number	$(7.0 \pm 0.7)10^3$
Natural linewidth	$(7.5 \pm 0.2)10^3$ Hz
Maximum output power	
Single-mode operation	50 μW
Multimode operation (2% transmissivity)	650 μW

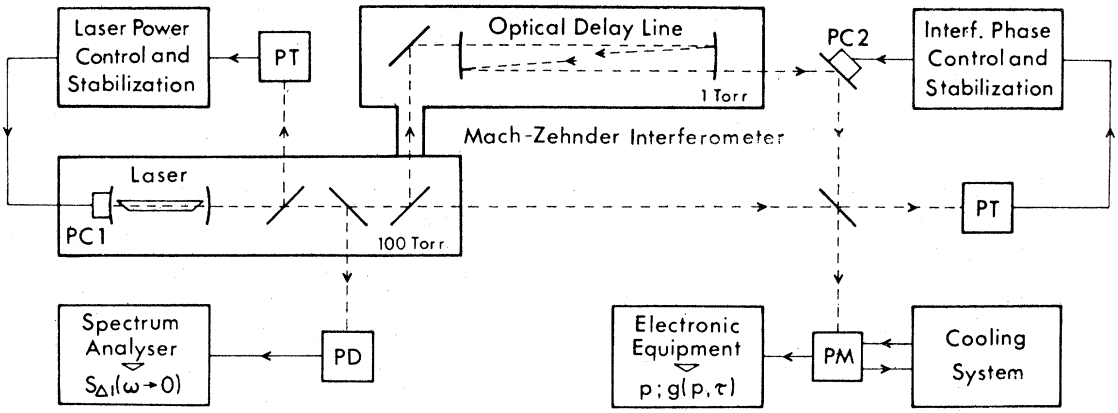

FIG. 2. Measuring system.

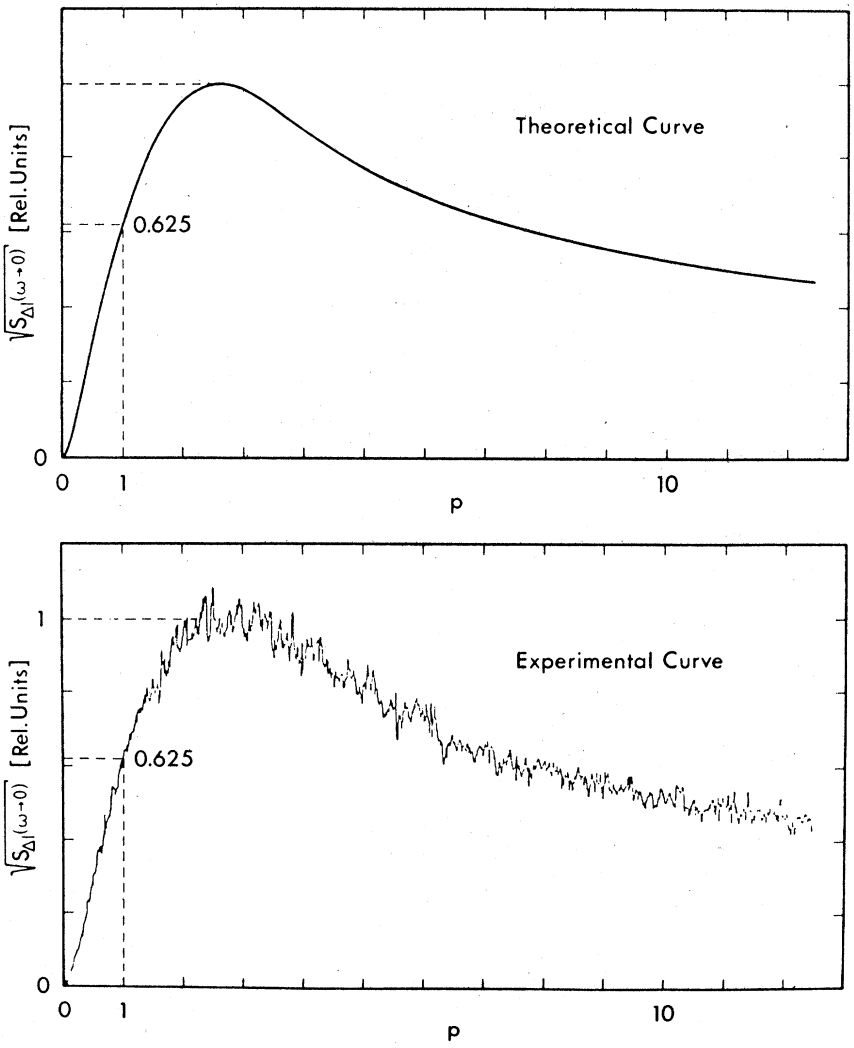

FIG. 3. Spectral power density of the natural intensity fluctuations near zero frequency $S_{\Delta I}(\omega \to 0)$ as a function of the laser operating point. Experimental curve measured for $\omega = 225$ Hz.

delay line inserted into the interferometer allows light paths up to 2000 m. A Mach-Zehnder interferometer is used, because backscatter to the laser, which may produce severe phase instabilities, must be avoided by all means. The output signal of the interferometer is measured by the photomultiplier PM behind a pinhole. To enable a quick controlled setting of the interferometer operating point, the phase difference between the partial beams can be shifted by means of a piezoelectric translator (PC2). For light paths shorter than 500 m, as long as the overall stability is sufficient, the operating point is kept constant by an intensity stabilization at an edge of the complementary interference figure.

The electronic system is designed to measure the normalized field autocorrelation function with high accuracy and signal-to-noise ratio, especially in the range $\gamma \lesssim 1$. According to Eq. (15), $\{I_{max}+I_{min}\}$ has to be measured directly. This is achieved by modulating the interferometer phase with a square function of the swing $\frac{1}{2}\pi$ by means of PC2. By choice of the correct interferometer operation point, a lock-in amplifier measures the values $\{I_{max}+I_{min}\}$, which is stabilized to 1 V by an automatic-gain-control-circuit. A second lock-in amplifier, using the same controlled ac preamplifier but a different reference signal, measures always $2I_{min}$ and hence $1-\gamma(\tau)$. In connection with the automatic control of the interferometer operating point, a continuous measurement of $\gamma(\tau)$ is accomplished. For path differences above 500 m the stability of the long light beam does not suffice to use the method described above. In this case the intensity of the two arms and I_{min} are measured successively and $\gamma(\tau)$ is computed according to Eq. (14).

V. MEASUREMENT RESULTS

Measurements of the normalized field auto correlation function $g(p,\tau)$ were made for seven delay

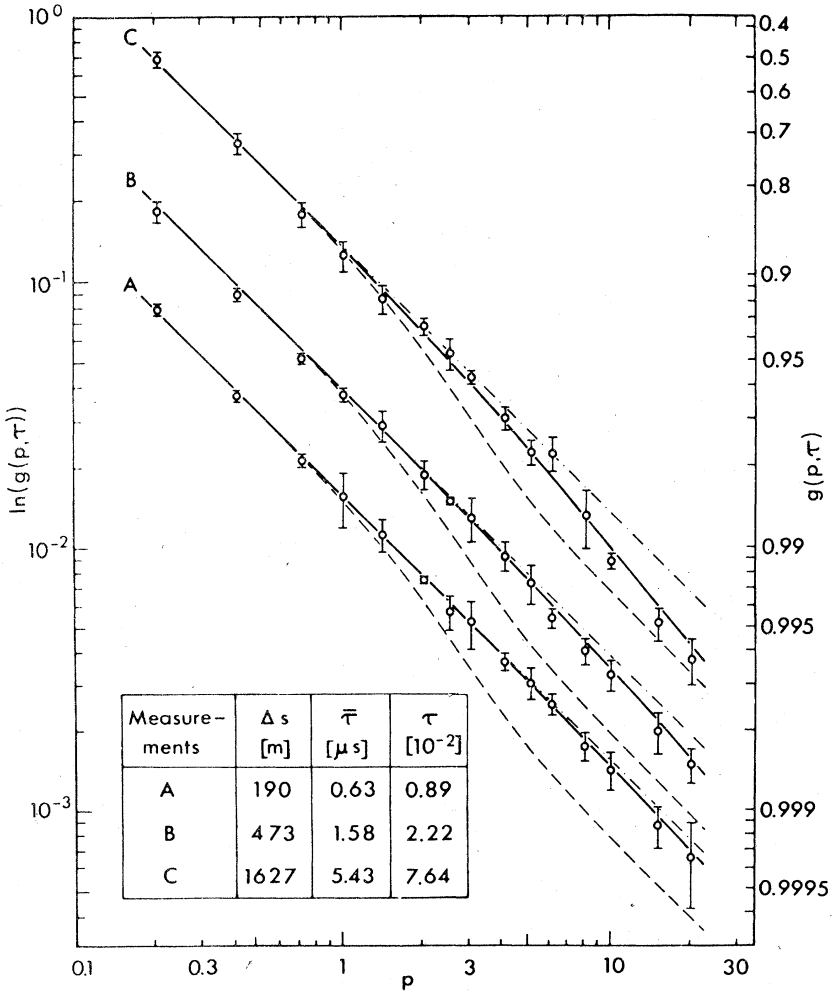

FIG. 4. Operating point dependence of the normalized field autocorrelation function.

times corresponding to path differences in the range between 80 and 2068 m and 14 laser operating points in the whole threshold region between $p = 0.2$ and $p = 20$. A representative choice of the experimental results is given in this section.

In Fig. 4 the measured values of $g(p, \tau)$ are shown as a function of the normalized laser output power p for three delay times τ. The technical influence has been eliminated according to Eq. (16), the approximate values of $g(p_r, \tau)$ for $p_r = 100$ were obtained by extrapolating the theoretical results derived for the region close to the threshold. Each point in Fig. 4 is the mean value of five independent values, the bars indicate its mean statistical error. The observed experimental scatter is clearly caused by nonstationary technical disturbances, i.e., by real changes of the visibility. Nevertheless, the statistical accuracy achieved is quite pronounced. For example, for a path length of 190 m and $p \geq 6$, the relative errors are less than 0.025%.

Figure 4 gives an immediate first qualitative indication of the nonexponential decay of the field autocorrelation function. For a pure exponential, the values corresponding to different delay times should emerge by parallel displacement in the selected nonlinear representation, independent of the special operating point dependence. This is surely not true for $p > 1$. The slope of roughly -1 fixed by the individual measuring point families refers to the general $1/p$ dependence of the natural linewidth.

The full curves in Fig. 4 are the complete theoretical solutions fitted to the experimental values by proper choice of the scaling factors C defined in Sec. I, whereas the broken curves are valid for pure Lorentz spectra of the width $\gamma_0(p)$. The dash-dotted straight lines extrapolate the behavior below threshold; they would be valid, if the laser light would not change its statistical character in the threshold region.

The measured values of $g(p, \tau)$ as shown in Fig. 4 were used to compute improved values with reduced statistical errors by means of a smoothing procedure after a suitable transformation. Minor differences of the individual scaling factors C_i were corrected by modifying all values according to the transformation $C_i \rightarrow \langle C \rangle$, thus allowing a meaningful combination of the values corresponding to different delay times. A systematic τ dependence excluding this procedure is not evident. The scatter of the scaling factors is explained by cleanings and adjustments of the resonator mirrors between the individual series of measurements causing small variations of the laser parameters β and q.

Figure 5 shows the time dependence of the experimental values of $g(p, \tau)$ for three operating

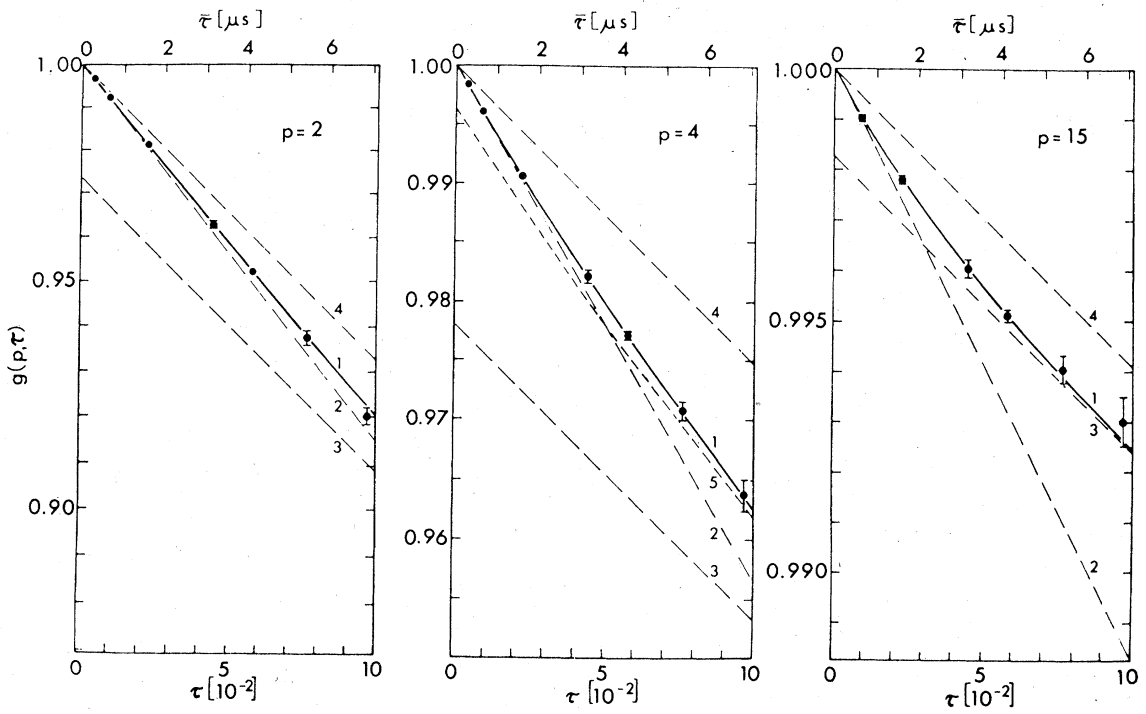

FIG. 5. Decay of first-order correlations for three operating points slightly above threshold. $[g_1(p, \tau) = \sum_m V_m \times \exp(-\lambda_m \tau), g_2(p, \tau) = 1 - \sum_m V_m \lambda_m \tau, g_3(p, \tau) = V_0 \exp(-\lambda_0 \tau), g_4(p, \tau) = \exp(-\lambda_0 \tau), g_5(p, \tau) = \sum_{0,1} V_m \exp(-\lambda_m \tau)]$.

points in the most interesting region above threshold together with the theoretical curves 1 and their asymptotes for $\tau \to 0$ and $\tau \to \infty$, curves 2 and 3. Pure Lorentz lines of the widths λ_0 would result in the curves 4. The experimental points are in reasonable agreement with curve 1, supporting the theoretical solution derived from the Van der Pol laser model. The integral contributions of the higher-order terms are indicated as differences between the curves 1 and 3. For $p = 15$ these terms are nearly relaxed at the maximum delay time of 7 μsec.

The existence of terms higher than first order can reliably be detected, as can be seen by comparing curve 5, representing the sum of the two lowest-order contributions for $p = 4$, with curve 1.

The clear proof of the nonexponential decay of the normalized field autocorrelation function $g(p, \tau)$, becoming visible by the nonlinear behavior in the half-logarithmic presentation in Fig. 5, was a challenge to isolate single exponential terms and to determine their parameters. The applied approximation scheme[26] delivers relaxation rates without initial arguments, the weight factors are obtained by the least-squares method. However, points with equidistant τ coordinates are required, which had to be determined by an interpolation procedure. In Fig. 6 the computed parameter values are compared with the theoretical solutions. The λ_0 values confirm excellently the $1/p$ dependence of the natural linewidth below and above threshold and the linewidth factor transition from 2 to 1 in the threshold region. The parameters of the higher-order terms, as far as they were obtained, show a satisfying agreement, too.

In addition to the normalized relaxation rates, the corresponding unnormalized linewidths (full widths at half power) in Hz are given in Fig. 6. The natural linewidth varies in the investigated power range between 200 and 40 000 Hz; at threshold it is 7475 Hz. Thus, the maximum spectral resolution achieved in this experiments is 2.3×10^{12}. The width of the technical Gaussian line was found to be about 10 000 Hz and hence a factor of 50 higher than the natural linewidth at $p = 20$.

VI. DISCUSSION

The results of our measurements demonstrate the physical reality of the fine structure of the field autocorrelation function predicted by the Van der Pol laser mode'. It would be of interest to know the mechanisms responsible for the individual terms. From the numerical computer solutions for the threshold region this information can not be deduced; nonetheless some simple conclusions are possible sufficiently far above threshold.

Essentially, the behavior of the field autocorrelation function $g(p, \tau)$ and hence the behavior of the parameters $V_m(p)$ and $\lambda_m(p)$ is determined by two effects, the increase of the resonator lifetime with rising stimulated emission rate, and the amplitude

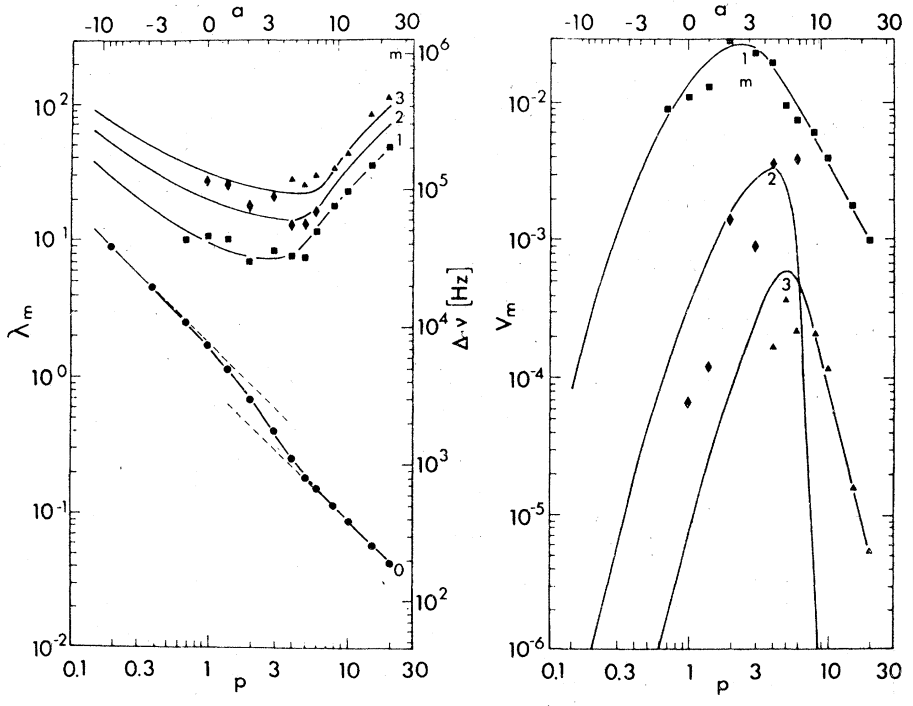

FIG. 6. Experimental values of the normalized and unnormalized linewidths λ_m and $\Delta\nu_m$, respectively, and the weight factors V_m.

stabilization due to the saturation of the inversion taking place above threshold. The first effect is clearly responsible for the general $1/p$ dependence of λ_0 and the second one for the linewidth factor transition and the higher-order fine structure terms. Well below threshold, when the cubic term in Eq. (1) is negligible, only the relaxation rate λ_0 is present. The same is approximately true far above threshold, where the small natural-amplitude fluctuations may be neglected. Evidently, the fine structure is associated with an incomplete amplitude stabilization; in the limit of lacking or total stabilization it disappears.

As a consequence of the amplitude stabilization, the laser signal above threshold can be interpreted as a sinusoidal carrier modulated by quantum phase noise and the remaining small portion of the quantum amplitude noise. The corresponding normalized field-autocorrelation function $g'(\tau)$ is found to be

$$g'(\tau)=(1/\bar{n}^2)[\gamma^2+\langle\rho^2\rangle g_\rho(\tau)]g_\Phi(\tau)\,, \tag{22}$$

if correlations between phase and amplitude fluctuations are neglected.

For $p\gg 1$ approximate expressions for $g_\Phi(\tau)$ and $g_\rho(\tau)$, the contributions of phase and amplitude fluctuations alone, can easily be obtained by a quasilinear solution of Eq. (1).[5] Both are exponential functions with the decay constants $\lambda_\Phi=1/a$ and $\lambda_\rho=2a$, respectively, ($a\simeq 2p/\sqrt{\pi}$ for $p\gg 1$). The weight factors and relaxation rates of the resulting double exponential function $g'(\tau)$ are

$$V_0'=\frac{2a^2}{2a^2+1}\,,\quad V_1'=\frac{1}{2a^2+1}\,,\quad \lambda_0'=\frac{1}{a}\,,\quad \lambda_1'=2a+\frac{1}{a}\,. \tag{23}$$

For $a=10$ the numerical values coincide fairly well with the corresponding exact values[7] given in brackets: $V_0'=0.9950$ (0.9950), $V_1'=4.975\times 10^{-3}$ (4.829×10^{-3}), $\lambda_0'=0.1$ (0.102 12), $\lambda_1'=20.1$ (19.237). Obviously, the lowest-order term of the field autocorrelation function is mainly determined by phase fluctuations and the first-order term by amplitude fluctuations, at least far above threshold.

Indications of the existence of terms higher than first order can be derived from the intensity correlation function $G_2(\tau)$ known from Refs. 5 and 7. From the relation

$$G_2(\tau)=4\gamma^2\langle\rho^2\rangle g_\rho(\tau)+G_{2\rho}(\tau)\,, \tag{24}$$

with $G_{2\rho}(\tau)=\langle\rho^2(t)\rho^2(t+\tau)\rangle-\langle\rho^2(t)\rangle^2$ follows

$$g_\rho(\tau)\simeq g_2(\tau)=G_2(\tau)/G_2(0) \tag{25}$$

for $p\gg 1$. Thus, $g_\rho(\tau)$ like $g_2(\tau)$ is composed of a series of exponentials and is approximately determined by the same set of parameters. Although the individual parameters differ from the exact ones, the function $g(\tau)$ is nevertheless reasonably approximated by $g'(\tau)$ obtained in this way. Because of a near pairwise degeneration of the decay constants[7] of $g_2(\tau)$ it is obvious to combine the corresponding terms and to compute effective parameters. As a consequence, even terms in $g'(\tau)$ cannot be expected, a prediction that is supported by the strong dominance of the odd terms in the exact solution (see. Fig. 1).

For $a=10$ the effective relaxation rates and weight factors V_0' and V_1' agree sufficiently with the exact values, whereas V_3' and V_5' differ by approximately a factor of 2 or 3, respectively. Discrepancies in this order of magnitude are not surprising because of the neglect of the small terms in Eq. (25) and the restriction leading to Eq. (22). With increasing distance from threshold a better agreement can be expected.

In the usual operating range of a laser far above threshold, the fine structure of the natural field autocorrelation function is thus essentially associated with an analogous structure of the natural amplitude correlation function resulting directly from the inherent nonlinearity of the laser process. Near threshold the values of the fine-structure parameters are influenced by couplings of phase and amplitude fluctuations.

Thus far we have made the premise that the theoretical results presented in Sec. II are directly applicable to the laser used for the measurements. Because some of the assumptions of the theoretical model are not fulfilled (e.g., the laser transition is not strongly homogeneously broadened and standing waves instead of travelling waves are present), a short justification shall be given. Specific laser properties as line broadening and field structure may be very important for the behavior of the laser far above threshold; near threshold, however, only modifications of the scaling factors β and q have to be allowed for.[7,27] The validity of the Van der Pol model is predicted to apply in the range $1/n_s<p<n_s$, where n_s is the averaged threshold photon number.[7] In our case n_s is approximately 7000 and thus by far greater than the maximum relative laser power $p=100$.

VII. CONCLUSIONS

Autocorrelations of the laser field yield information about natural amplitude and phase fluctuations as well. Although effects connected with phase fluctuations are of fundamental physical interest, especially near the oscillation threshold, most experimental work was concentrated on intensity correlation and related quantities. This may be explained by the great difficulties arising from un-

avoidable technical noise that affects the phase of the field far more than the amplitude and the intensity. As a consequence, the natural component is in general masked largely by technical phase noise. Using an improved interferometric autodyne method and an experimental system optimized in decisive aspects, we have made measurements of the natural field autocorrelation function throughout the threshold region. The stationary component of the technical fluctuations was eliminated by a reference-measuring technique taking advantage of the different operating-point dependence of technical and natural noise. Additional sporadic disturbances, however, turned out to be troublesome; they result in a spread of the measured values and in a small fraction of useful measurements.

Nevertheless, the achieved accuracy is sufficient to confirm the nonexponential decay of field autocorrelations predicted by the Van der Pol laser model and to compute parameters of some of the exponential fine-structure terms characterizing the special shape of the field autocorrelation function. Implicitly, small deviations of the natural laser spectrum from a pure Lorentz profile slightly above threshold are detected. The higher-power density in the wings results from a flat, broad contribution which is closely associated with a partial stabilization of the field amplitude due to the nonlinear character of the laser process. Above threshold a narrowing of the natural linewidth up to a factor of 2 in addition to the general reciprocal power dependence is observed, in full agreement with the theory.

---

*Present address: Carl Zeiss, 7082 Oberkochen, Federal Republic of Germany.

[1]H. Risken and H. D. Volmer, Z. Phys. 201, 323 (1967).
[2]H. Risken and H. D. Volmer, Z. Phys. 204, 240 (1967).
[3]H. Risken, in *Progress in Optics*, edited by E. Wolf (North-Holland, Amsterdam, 1970), Vol. VIII, p. 241.
[4]H. Risken, Fortschr. Phys. 16, 261 (1968).
[5]K. Seybold and H. Risken, Z. Phys. 267, 323 (1974).
[6]M. Lax and W. H. Louisell, IEEE J. Quantum Electron. QE-3, 47 (1967).
[7]R. D. Hempstead and M. Lax, Phys. Rev. 161, 360 (1967).
[8]M. Lax and M. Zwanziger, Phys. Rev. A 7, 750 (1973).
[9]S. Chopra and L. Mandel, *Coherence and Quantum Optics*, edited by L. Mandel and E. Wolf (Plenum, New York, 1973), p. 805.
[10]S. Chopra and J. P. Dudeja, Optica Acta 23, 37 (1976).
[11]The authors of Ref. 10 compare the measured parameters with values that are not exactly identical with the theoretical results given in Ref. 7. The agreement is slightly better if these results are considered. The experimental parameter M_1 seems to be reproduced incorrectly. A weight factor sum of 0.9 is not justified by the experimental data.
[12]M. Corti, V. Degiorgio, and F. T. Arecchi, Opt. Commun. 8, 329 (1973).
[13]M. Chopra and L. Mandel, Phys. Rev. Lett. 30, 60 (1973).
[14]M. Corti and V. Degiorgio, Opt. Commun. 11, 1 (1974).
[15]D. Meltzer, W. Davis, and L. Mandel, Appl. Phys. Lett. 17, 242 (1970).
[16]E. Jakeman, C. J. Oliver, E. R. Pike, M. Lax, and M. Zwanziger, J. Phys. A 3, L52 (1970).
[17]H. Gerhardt, H. Welling, and A. Güttner, Z. Phys. 253, 113 (1972).
[18]A. E. Siegman, B. Diano, and K. R. Manes, IEEE J. Quantum Electron. QE-3, 180 (1967).
[19]A. E. Siegmann and R. Arrathoon, Phys. Rev. Lett. 20, 901 (1968).
[20]R. Arrathoon and A. E. Siegman, J. Appl. Phys. 40, 910 (1969).
[21]K. R. Manes and A. E. Siegman, Phys. Rev. A 4, 373 (1971).
[22]Yu. I. Zaitsev and D. P. Stepanov, Zh. Eksp. Theor. Fiz. 55, 1645 (1968) [Sov. Phys. JETP 28, 863 (1969)].
[23]E. D. Hinkley and C. Freed, Phys. Rev. Lett. 6, 277 (1969).
[24]H. Z. Cummins and H. L. Swinney, in *Progress in Optics*, edited by E. Wolf (North-Holland, Amsterdam, 1970), Vol. VIII, p. 135.
[25]M. Born and E. Wolf, *Principles of Optics* (Pergamon, New York, 1970).
[26]C. E. Fröberg, *Introduction to Numerical Analysis* (Addison-Wesley, Reading, Mass, 1965).
[27]A. P. Kanzantsev and G. I. Surdutovich, Prog. Quantum Opt. 3, 231 (1974).